A role for the Adenomatous Polyposis Coli protein in chromosome segregation

Kenneth B. Kaplan*†, Aurora A. Burds*, Jason R. Swedlow‡, Songül S. Bekir‡, Peter K. Sorger* and Inke S. Näthke‡§

*Department of Biology, Massachusetts Institute of Technology, Cambridge, Massachusetts 02139, USA
‡School of Life Sciences, University of Dundee, Dundee DD1 5EH, UK
†Current address: Section of Molecular and Cellular Biology, University of California Davis, Davis, California 95616, USA
§e-mail: i.s.nathke@dundee.ac.uk

Mutations in the Adenomatous Polyposis Coli (*APC*) gene are responsible for familial colon cancer and also occur in the early stages of sporadic colon cancer[1]. APC functions in the Wnt signalling pathway to regulate the degradation of β-catenin (reviewed in refs 1–3). APC also binds to and stabilizes microtubules *in vivo* and *in vitro*[4], localizes to clusters at the ends of microtubules near the plasma membrane of interphase cells[5,6], and is an important regulator of cytoskeletal function[7,8]. Here we show that cells carrying a truncated *APC* gene (*Min*)[9] are defective in chromosome segregation. Moreover, during mitosis, APC localizes to the ends of microtubules embedded in kinetochores and forms a complex with the checkpoint proteins Bub1 and Bub3. *In vitro*, APC is a high-affinity substrate for Bub kinases. Our data are consistent with a role for APC in kinetochore–microtubule attachment and suggest that truncations in APC that eliminate microtubule binding may contribute to chromosomal instability in cancer cells[10].

To determine whether cells carrying mutant APC segregate chromosomes correctly, clonal cultures of wild-type embryonic stem (ES) cells and ES cells carrying *Min* APC (Fig. 1a) were karyotyped after 10–20 generations. In *Min* but not wild-type ES cells, there were a significant number of chromosomes near the spindle equator, some of which appeared torn, even when the bulk of the chromosomes had moved to the spindle (Fig. 1b, c). The chromosome number in *Min* ES cells was highly variable, indicating that aneuploid cell divisions had occurred (Fig. 1d). In contrast, the chromosome number in wild-type cells clustered tightly around 38 (the diploid autosome number; Fig. 1d). We conclude that the *Min* mutation promotes genome instability in ES cells by diminishing the fidelity of chromosome segregation.

To determine how APC might function in mitosis, we stained asynchronous HeLa and PtK cells with antibodies against tubulin, APC and core kinetochore proteins (using CREST antisera[11]). Three-dimensional views of nuclear morphology were generated by optical sectioning microscopy followed by iterative deconvolution (using an Applied Precision DeltaVision microscope). In mitotic cells we observed discrete foci of APC staining at kinetochores, centrosomes and, to a varying extent, in the cytoplasm (Fig. 2; and data not shown). APC staining at kinetochores was directly adjacent to sites of CREST staining at the ends of microtubules (Fig. 2c, d). Most, if not all, microtubule-bound kinetochores seemed to be associated with APC. Neither β-catenin nor plakoglobin staining was detected at kinetochores (data not shown), suggesting that kinetochore-associated APC is not in a complex with either of these proteins.

To determine the point during the cell cycle at which APC binds to kinetochores, cells expressing Bub3–green fluorescent protein (GFP) were stained with antibodies against APC at various stages of mitosis. Bub3 is present at high levels on kinetochores during prophase, falls about threefold as microtubules become attached during prometaphase, and dissociates late in anaphase[12]. In prophase cells, foci of kinetochore-bound Bub3 were rarely associated with APC foci, which were scattered throughout the cell (Fig. 2e, f; the distance between Bub3 and APC foci was at least 0.8 μm).

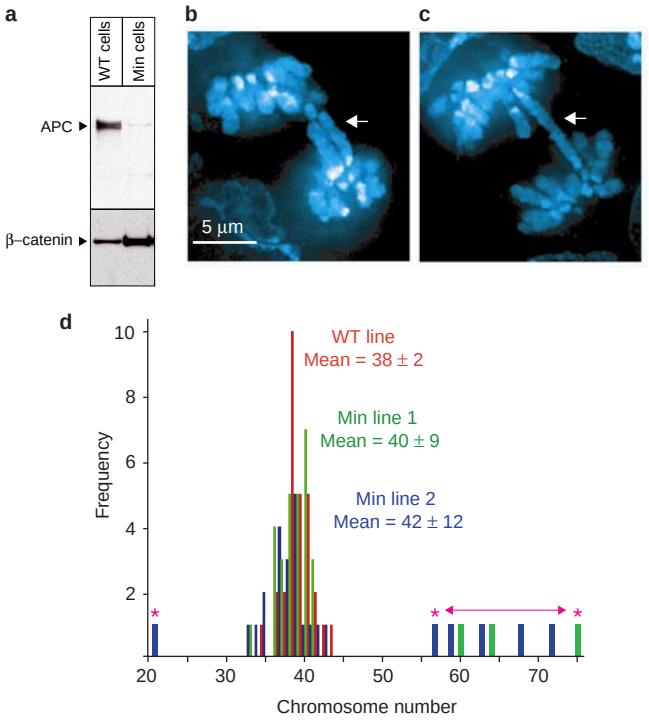

Figure 1 **Cells lacking functional APC protein undergo aberrant mitosis. a**, *Min* ES cells lack full-length APC. Whole-cell lysates were prepared from stem cells containing mutations in both copies of APC (*Min* ES cells), or from wild-type ES cells, and equal amounts of protein analysed by western blotting with anti-APC and anti-β-catenin antibodies. *Min* cells have elevated levels of β-catenin, as expected. **b**, **c**, Mitotic errors in *Min* ES cells as visualized by DAPI. In 7 out of 21 *Min* ES cells (but only 1/25 wild-type cells) in which most chromosomes had segregated to the poles, some chromosomes remained at the midzone (white arrows). **d**, Aneuploidy in *Min* ES cell. A wild-type ES cell line and two independent *Min* lines were cultured for 10 passages, and the number of autosomes determined for 20–30 cells from each line. Asterisks denote highly aneuploid cells.

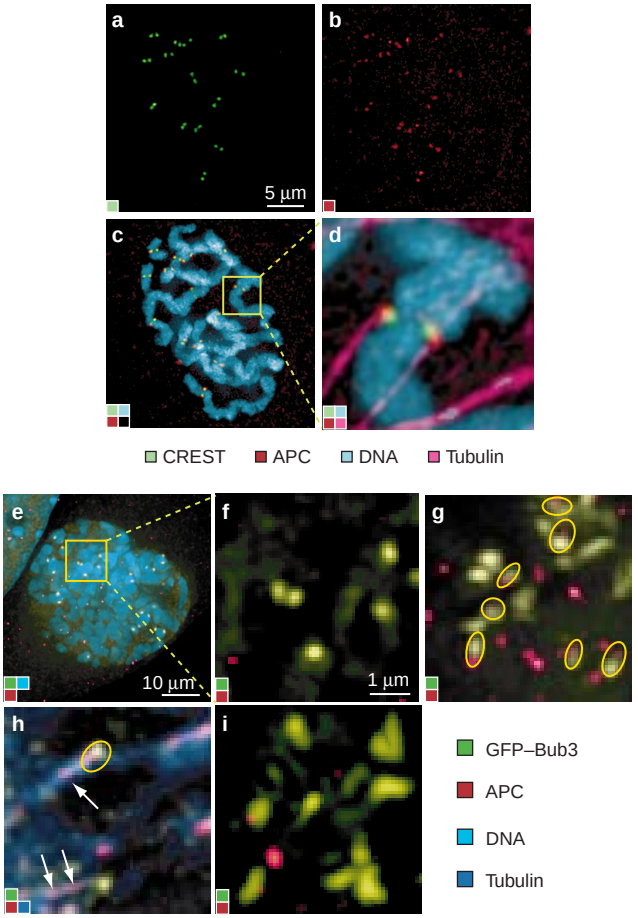

Figure 2 **APC is localized to kinetochores in mitotic cells. a–c**, Projections of 3D reconstructions of mitotic PTK cell stained with CREST to visualize kinetochores (green), anti-APC (red) and DAPI (blue). Staining of APC was also observed at centrosomes, which were located to the left and right of the chromosomes in these images. Similar staining was observed in HeLa cells, but the levels of cytoplasmic APC were generally higher. Antiserum from four different rabbits showed a similar pattern of staining, but pre-immune sera and anti-APC serum depleted by incubation with antigen did not (not shown). **d**, A ×32 magnification of the area outlined by the yellow box in **c**. Tubulin staining (magenta) is also shown. APC association with kinetochores requires microtubules. 3T3 cells expressing GFP–Bub3 (green) were stained with anti-APC (red), DAPI (blue) and anti-tubulin (dark blue) as indicated. **e**, **f**, Prophase cell at low (**e**) and high (**f**) magnification with the DAPI channel suppressed. The mean distance between APC and Bub3 foci was 0.61± 0.18 μm (n = 43). **g**, Prometaphase cell with sites of APC and Bub3 colocalization circled in yellow; APC and Bub3 foci are separated by 0.3 ± 0.1 μm (n = 19). **h**, A metaphase cell in which Bub3–GFP and APC are seen to colocalize at the ends of microtubules, but APC is also visible along the length of microtubule fibres (white arrows). **i**, A cell arrested in pro-metaphase by treatment with 30 μM nocodazole for 1 h. Sites of APC and GFP–Bub3 colocalization are absent, as judged by an increase in the mean distance between APC and GFP–Bub3 signals to 1 ± 0.2 μm (n = 56). Scale bars are identical in **f**, **g**, **h**, **i**.

In prometaphase cells, two populations of APC foci were seen: one far from Bub3 (> 1 μm); and one close to Bub3 (in the examples circled in Fig. 2g, the centre-to-centre distances were 0.3 ± 0.1 μm). The latter class included APC foci that were adjacent to low-intensity Bub3–GFP signals, indicating that these kinetochores were bound to microtubules. Consistent with this idea, APC was bound in metaphase cells to the ends of microtubules immediately adjacent to Bub3–GFP and along kinetochore microtubules (Fig. 2h, white arrows).

To determine whether the localization of APC to kinetochores is dependent on microtubules, cells were treated with the microtubule poison nocodazole. This causes microtubules to depolymerize and cells to arrest in mid-metaphase. We observed that APC and Bub3–GFP foci were no longer adjacent at kinetochores in nocodazole-treated cells (Fig. 2i). Quantitation yielded an average separation of 0.8–1.2 μm, similar to that observed in prophase. We conclude that the binding of APC to kinetochores requires intact microtubules and that APC concentrates at the ends of microtubules embedded in kinetochores.

The juxtaposition of APC and Bub complexes led us to examine whether these proteins interact. We found that APC co-immunoprecipitated with both Bub1 and Bub3 from the lysates of mitotically arrested, but not asynchronous HeLa cells (Fig. 3b). The interaction between Bub proteins and APC was confirmed using recombinant proteins produced in insect cells (data not shown). The small fraction of APC that is associated with Bub proteins in mitotic cell lysates (2–5% of total APC in lysate) may reflect the loss of microtubules in the nocodazole-arrested cells, as microtubules are required for the localization of APC to kinetochores (Fig. 2i). Although cell extracts derived from nocodazole-arrested cells support APC–Bub interactions, this may only represent a small fraction of the amount of APC–Bub complex found in a mitotic cell with intact microtubules.

We next determined whether APC might be a substrate for Bub kinases. Bub3 and epitope-tagged Bub1 or BubR1 were co-expressed in insect cells, the kinases isolated on beads and kinase reactions performed using Bub1/R1-bound beads, [γ-^{32}P]ATP and a central fragment of APC (M-APC; Fig. 3c). Recombinant complexes containing Bub1–Bub3 or BubR1–Bub3, and also Bub1 isolated from mitotic HeLa cells, phosphorylated APC with an efficiency of 2–4 mol of phosphate per mol of APC (Fig. 3d; and data not shown). As a control for contaminating kinases, *in vitro* reactions with recombinant Bub1/R1 kinases carrying lysine to arginine mutations in the ATP-binding pocket (hBub1K821R or hBubR1K795R) were much less active in APC phosphorylation (Fig. 3c, lane 3; and data not shown). As a specificity control, we compared the ability of Bub1 (or BubR1) to phosphorylate APC, with its ability to phosphorylate casein and myelin basic protein (MBP), two classical kinase substrates. We observed high specificity for APC, with half-maximal phosphorylation of APC by Bub1 at 5 nM, compared with half-maximal phosphorylation of casein and MBP at concentrations 100–150 times higher (Fig. 3d; and data not shown). We conclude that Bub1–Bub3 and BubR1–Bub3 kinase complexes can phosphorylate APC efficiently *in vitro* and with very high specificity.

Among the kinases that have been shown to modify APC, glycogen synthase kinase 3β (GSK3β) is particularly interesting because its activity is regulated by Wnt signalling[3]. Bub1 phosphorylation sites were found in both the middle and carboxy-terminal fragments of APC, interspersed with predicted GSK3β sites (data not shown). When the kinase activity of Bub1 on a de-phosphorylated M-APC fragment was compared with its activity on the same fragment re-phosphorylated with GSK3β, the GSK3β-modified APC fragment was a 5-fold better substrate than phosphatase-treated APC over a 20-fold range of substrate concentrations (Fig. 3e). These data indicate that GSK3β phosphorylation may promote subsequent phosphorylation of APC by Bub kinases.

The interaction of APC with the Bub checkpoint complexes raised the possibility that APC might be a component of the spindle checkpoint. We therefore challenged colonic tumour cell lines carrying either wild-type or mutant APC with the microtubule poison taxol, and assayed the extent to which they arrest in mitosis by fluorescence-activated cell sorting (FACS). Cells containing wild-type (HCT116) or mutant APC (HT29) arrested with a 4N DNA content after 6–9 h in taxol (Fig. 4a). Some cell lines appeared to arrest less well (SW480), but we thought that this might be caused by factors unrelated to APC status. We therefore probed checkpoint function in explanted *Min/Min* and wild-type blastocysts from congenic animals.

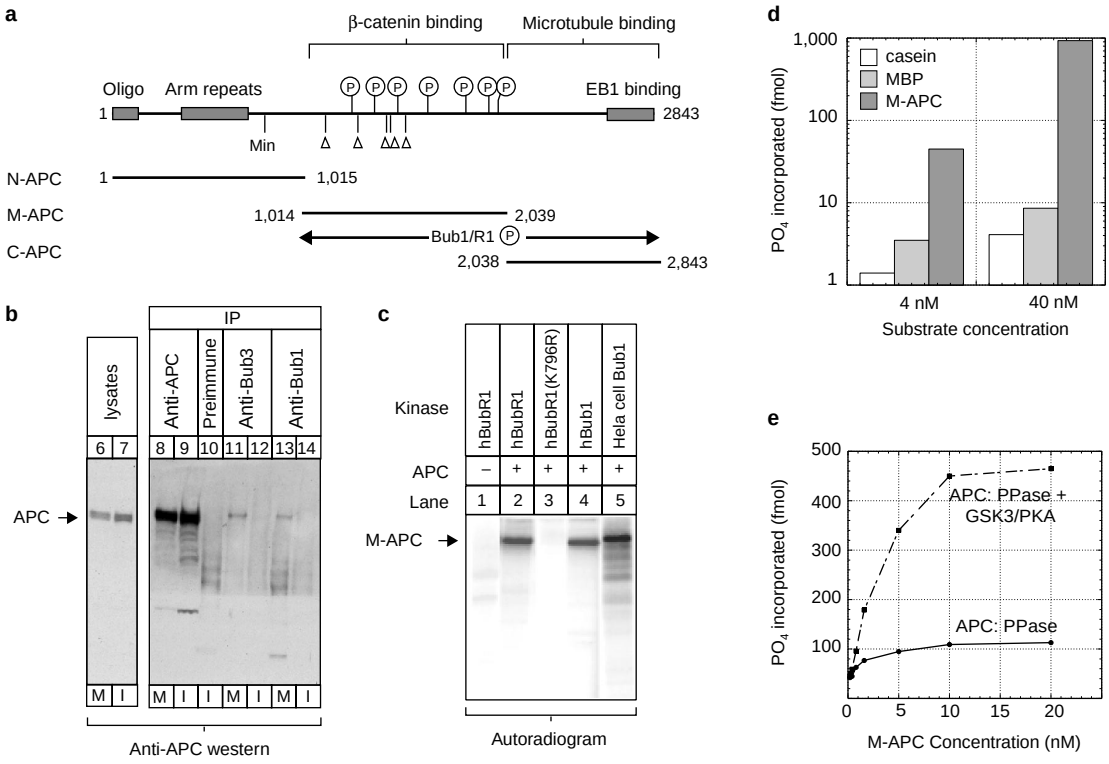

Figure 3 **Bub kinases specifically phosphorylate and bind to APC. a**, The sequence of APC with functional domains outlined. 'Oligo' denotes the oligomerization domain, 'Arm repeats' denotes the armadillo repeats and 'EB1' denotes the binding site for the EB1 protein. 'P' indicates predicted sites of GSK3β phosphorylation, triangles indicate the five truncations most commonly found in colon cancers (as determined from the APC mutation database; http://perso.curie.fr/Thierry.Soussi/APC.html), and the nonsense mutation at codon 850 in the *Min* mouse[9] is indicated (Min). Fragments of APC used for phosphorylation and binding studies are also shown. **b**, APC co-immunoprecipitates with Bub1 and Bub3 in extracts from mitotic HeLa cells. Hela cells arrested in 200 ng ml^{-1} nocodazole for 12 h were lysed in detergent, and analysed by immunoprecipitation using anti-APC, anti-Bub1 and anti-Bub3 antibodies. Immune complexes were analysed on western blots with anti-APC antibodies. **c**, Phosphorylation by Bub1 and BubR1. *In vitro* kinase reactions were performed with recombinant M-APC (see **a**) and recombinant Bub1–Bub3 or BubR1–Bub3 complexes or HeLa cell Bub1–Bub3 as indicated. As a demonstration of kinase specificity, mutants altered in residues critical for phosphate transfer[18] were analysed (hBubR1K796R, lane 3; and hBub1K821R, not shown). The amount of phosphate incorporated was determined by phosphorimager analysis of SDS–PAGE gels. **d**, Bub kinase substrate specificity. *In vitro* kinase reactions were performed as in **c** using casein, myelin basic protein (MBP) or M-APC as substrates. **e**, APC phosphorylated by GSK3β is a better substrate for Bub kinase. Recombinant M- APC generated in insect cells was dephosphorylated using lambda-phosphatase (PPase) and either used directly, or first phosphorylated with purified PKA and GSK3β as described[17]. APC concentrations varied from 1 to 20 nM, and the amount of phosphorylation was determined as in **d**.

Experiments with blastocysts lacking Mad2 (ref. 13) or Bub3 (ref. 14) have shown that both are required for the mitotic arrest of embryonic cells after microtubule depolymerization. We isolated blastocysts from intercrosses of *Min*/+ mice at embryonic day E3.5, treated the blastocysts at E5.5 with nocodazole and then stained them with antibodies against phosphorylated histone H3 to determine mitotic index. As a measure of S-phase index, the extent of 5-bromodeoxyuridine (BrdU) incorporation was also determined. A total of 16 embryos from 4 females were challenged with nocodazole, of which three were unambiguously *Min*/*Min* by polymerase chain reaction (PCR) genotyping. The fraction of mitotic cells was similar in these three knockout blastocysts and in wild-type littermate controls (Fig. 4b–d). From these data we conclude that *Min*/*Min* embryonic cells can arrest in mitosis in response to microtubule depolymerization and that, within the resolution of this assay, the mitotic checkpoint is functional.

Our data suggest that mutations in APC cause errors in chromosome segregation. Because APC is a (+)-end microtubule-binding protein and localizes to kinetochores, it seems reasonable to propose that APC stabilizes the plus ends of kinetochore microtubules and thereby aids in their attachment to chromosomes. The interaction of APC with Bub complexes is intriguing, although our data argue against a role for APC in the spindle checkpoint. Instead, we speculate that the phosphorylation of APC by Bub kinases is involved in regulating kinetochore–microtubule attachment. Indeed, phosphorylation of APC causes a decrease in its ability to bind microtubules[4]. It is, however, possible that APC or its associated proteins influence Bub checkpoint complexes, and thereby have a non-essential role in checkpoint signalling.

One important implication of our findings is that truncations in APC that eliminate microtubule binding may contribute to chromosome instability (the CIN phenotype) in colon cancer cells because they directly affect chromosome-spindle attachment. Phosphorylation of APC by Bub kinases may be an important aspect of this function, explaining why the loss of Bub1 kinase activity is a common feature of CIN cell lines[15]. Mapping and then disrupting the interaction between Bub kinases and APC should make it possible to test this hypothesis and to determine the physiological role of the APC–Bub kinase interaction.

Methods

Immunocytochemistry.

Cells were fixed in 3.7% paraformaldehyde for 15 min at 37 °C, permeabilized in 0.1% Triton X-100, 2% bovine serum albumin fraction V (Boehringer Mannheim) and 2% normal goat serum (Jackson

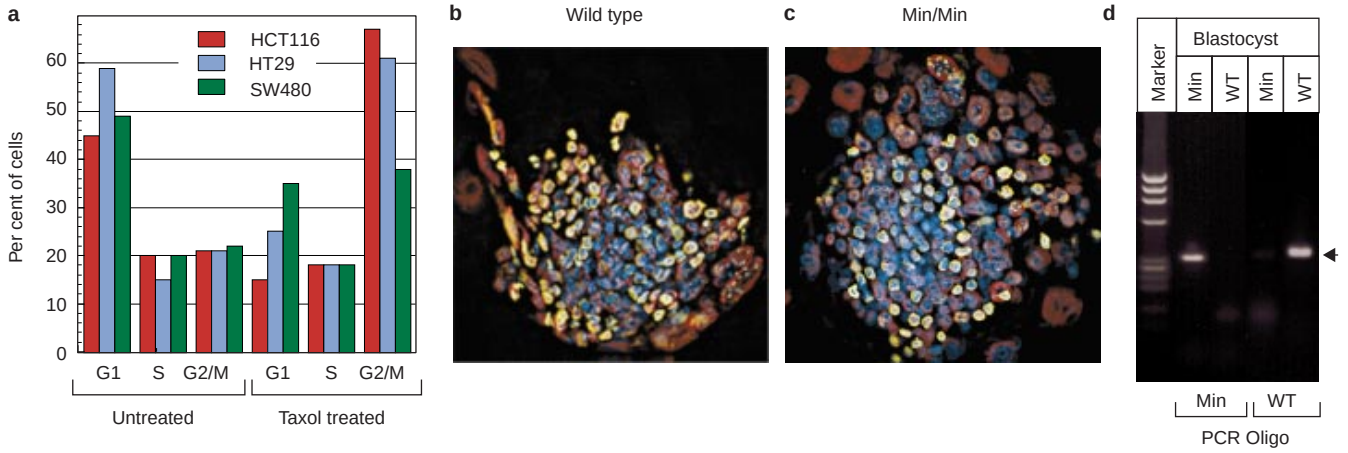

Figure 4 **Analysing the role of APC in the mitotic checkpoint. a**. Cell-cycle analysis by FACS of tumour cell lines carrying full-length APC (HCT116), or truncated APC (HT29, SW480). Cells were treated for 6–9 h with 5 ng ml^{-1} taxol before analysis. **b**, **c**, Analysis of mitotic arrest in whole-mount embryos with the indicated genotypes. Blastocysts were isolated from *Min/+* intercrosses and cultured *in vitro* to E5.5, and then treated with nocodazole and BrdU before being fixed, stained and imaged by deconvolution microscopy as described[13]. Anti-BrdU (red) shows S-phase index, anti-phospho H3 (yellow) shows mitotic index and DAPI (blue) shows all nuclei. **d**, Genotyping by PCR of embryos in **b** and **c** using allele-specific primers. DNA isolated from blastocysts was subjected to PCR using allele-specific primers to distinguish wild-type from *Min/Min* blastocysts.

ImmunoReserach) for 30 min. We stained cells with human CREST antisera (F. McKeon), rabbit polyclonal, affinity-purified anti-APC antisera[5] or mouse monoclonal anti-tubulin antibodies (DMA1 or TUB2.1; Sigma), followed by fluorescein isothiocyanate (FITC)-, Texas-red-, and Cy5-conjugated goat anti-human, anti-rabbit and anti-mouse secondary antibodies (Santa Cruz and Jackson ImmunoResearch). Chromosomes were stained with 4′,6-diamidino-2-phenylindole (DAPI; Sigma). A fusion of enhanced GFP to the amino terminus of Bub3 was introduced into 3T3 or HeLa cells expressing ecotrophic virus receptor, by infection with a retrovirus constructed from a pBabe–puromycin cassette[16]. We examined samples using a Zeiss-Applied Precision Delta Vision Restoration microscope as described[12].

Embryonic stem cells.

Mouse embryonic stem (ES) cell lines were kind gifts from R. Weinberg and A. Fazeli. For karyotyping, cells were arrested for 2 h with 10 nM taxol, treated with 75 mM KCl, fixed with methanol-acetic acid and dried in air overnight. Trypsinization was followed by Giemsa staining (BDH). We performed experiments with blastocysts as described[13].

Genotyping PCR protocol.

After immunofluorescence analysis, DNA was extracted from embryos grown in culture as described[13]. A region surrounding the *Min* locus was first amplified by PCR using oAB53 (5′-GCACTTGAAATCTCACAGCTTG-3′) and oAB59 (5′-GGTTTCATTTGGCCTCTTTTACC-3′). This was followed by re-amplification using nested, allele-specific primers. The wild-type primer set was oAB50 (5′-ACCTCGCTCTCTCTCCA-3′) and oIMR033 (Jackson laboratory website; http://lena.jax.org/resources/documents/imr/protocols/Apc(Min)_Chem.html). The Min-specific primer set was oIMR035 and oIMR758 (also from Jackson laboratory website). We ensured accurate genotyping by repeating amplifications twice.

Recombinant proteins and kinase assays.

Human Bub1 and BubR1 were cloned into baculovirus vectors as His_{10}HA (haemagglutinin A) fusions and co-expressed with murine Bub3 (which differs from human Bub3 at a single residue) in insect cells. Recombinant and endogenous HeLa cell Bub1/R1–Bub3 complexes were isolated by immunoprecipitation using protein-A–sepharose beads and anti-HA, anti-Bub3 or anti-Bub1 antibodies[12]. Beads were washed into 20 µl kinase buffer (20 mM Tris, pH 7.2, 5 mM $MgCl_2$ and 1 mM dithiothreitol) and incubated at 25 °C for 20 min in kinase buffer supplemented with 50 µM ATP, 30 µCi [^{32}P]ATP and myelin basic protein or α-casein (Sigma). We produced fragments of APC in insect cells as described[17]. Dephosphorylated and GSK3β re-phosphorylated M-APC was generated as described[17]. Briefly, M-APC fragment immobilized on an affinity resin was treated with λ-phosphatase (New England Biolab) before elution to generate de-phosphorylated M-APC. Similarly, we generated GSK3β re-phosphorylated APC by first treating the immobilized APC fragment with λ-phosphatase, then with PKA (to pre-phosphorylate M-APC, which is required for efficient phosphorylation with GSK3β[17]) and finally with GSK3β. The extent of phosphorylation was determined by phosphorimager analysis of SDS–PAGE gels.

RECEIVED 21 SEPTEMBER 2000; REVISED 30 NOVEMBER 2000; ACCEPTED 24 JANUARY 2001; PUBLISHED 22 MARCH 2001.

1. Kinzler, W. K. & Vogelstein, B. *Cell* **87,** 159–170 (1996).
2. McCartney, B. M. & Peifer, M. *Nature Cell Biol.* **2,** E58–E60 (2000).
3. Peifer, M. & Polakis, P. *Science* **287,** 1606–1609 (2000).
4. Zumbrunn, J., Inoshita, K., Hyman, A. A. & Näthke, I. S. *Curr. Biol.* **11,** 44–49 (2000).
5. Näthke, I. S., Adams, C. L., Polakis, P., Sellin, J. H. & Nelson, W. J. *J. Cell Biol.* **134,** 165–179 (1996).
6. Mimori-Kiyosue, Y., Shiina, N. & Tsukita, S. *J. Cell Biol.* **148,** 505–517 (2000).
7. McCartney, B. M. *et al. J. Cell Biol.* **146,** 1303–1318 (1999).
8. Yu, X., Waltzer, L. & Bienz, M. *Nature Cell Biol.* **1,** 144–151 (1999).
9. Su, L. K. *et al. Science* **256,** 668–670 (1992).
10. Lengauer, C., Kinzler, K. & Vogelstein, B. *Nature* **396,** 643–649 (1998).
11. Earnshaw, W. C. & Rothfield, N. *Chromosoma* **91,** 313–321 (1985).
12. Martinez Exposito, M., Kaplan, K., Copeland, J. & Sorger, P. *Proc. Natl Acad. Sci. USA* **96,** 8493–8498 (1999).
13. Dobles, M., Libertal, V., Scott, M. L., Benezra, R. & Sorger, P. K. *Cell* **101,** 635–645 (2000).
14. Kalitsis, P., Earle, E., Fowler, K. J. & Choo, K. H. *Genes Dev.* **14,** 2277–2282 (2000).
15. Cahill, D. P. *et al. Nature* **392,** 300–303 (1998).
16. Morgenstern, J. P. & Land, H. *Nucleic Acid Res.* **18,** 3587–3596 (1990).
17. Rubinfeld, B. *et al. Science* **272,** 1023–1026 (1996).
18. Hanks, S. K. & Junter, T. *FASEB J.* **9,** 576–596 (1995).

ACKNOWLEDGEMENTS

We thank the Marine Biological Laboratory, R. Weinberg, J. Copeland, the T. J. Mitchison laboratory and the Human Cytogenetics Group at Ninewells Hospital for help, and members of the I.S.N. laboratory and K. Storey for critical reading of the manuscript. A substantial portion of this work was carried out at UC Davis with the support of the American Cancer Society. This work was also supported by grants from the NIH and Merck (to P.K.S.) and from the Wellcome Trust and the Cancer Research Campaign (to J.R.S.), and by a Cancer Research Campaign Senior Fellowship and a Burroughs Wellcome Career Development Award to I.S.N.

Correspondence and requests for materials should be addressed to I.S.N.